Dendrimer-assisted low-temperature growth of carbon nanotubes by plasma-enhanced chemical vapor deposition†

Placidus B. Amama,*[a] Oluwaseyi Ogebule,[b] Matthew R. Maschmann,[ac] Timothy D. Sands[ad] and Timothy S. Fisher[ac]

Received (in Berkeley, CA, USA) 23rd February 2006, Accepted 8th May 2006
First published as an Advance Article on the web 2nd June 2006
DOI: 10.1039/b602623k

Using a shielded growth approach and N_2-annealed, nearly monodispersed Fe_2O_3 nanoparticles synthesized by interdendritic stabilization of Fe^{3+} species within fourth-generation poly(amidoamine) dendrimers, carbon nanotubes and nanofibers were successfully grown at low substrate temperatures (200−400 °C) by microwave plasma-enhanced chemical vapor deposition.

Carbon nanotubes (CNTs)[1] with either single (SWNTs) or multiple (MWNTs) walls and their less graphitized form, carbon nanofibers (CNFs), are extraordinary materials that have several potential applications, notably electron-field emission, electrochemical probes, membranes for microfluidic devices, and nanoelectronic devices.[2,3] However, the applications of CNTs to specific areas such as microelectronics packaging, macroelectronics, molecular electronics and integrated sensing devices will require the compatibility of CNT growth conditions with standard semiconductor processes. The typical CVD growth temperature range (600–1000 °C) precludes the use of temperature-sensitive substrates required for these applications. Growth temperatures in this range are too high because most metal contacts can only tolerate temperatures up to 450 °C for a limited time without significant loss of electrical performance.[2]

Plasma-enhanced chemical vapor deposition (PECVD) is capable of producing CNTs on appropriate catalyst-supported substrates at relatively low temperatures, as demonstrated by several authors.[2,4,5] Hofmann *et al.*[4] have shown that the presence of a highly reactive plasma environment decreases the activation energy of the CNT growth process. However, growth temperatures of CNTs could not be lowered below 600 °C using Mo/Co catalyst supported on nanoporous MgO or transition metal films. Most PECVD growth of CNTs/CNFs at low-temperatures (<500 °C) has been accomplished through the use of a bimetallic catalyst,[6,7] reactive carbon precursor,[4,8] low plasma power,[5a] controlled pressure,[7] and water[9] or hydrocarbon[5d] plasma. The literature reveals very few studies on shielded growth of CNTs by PECVD. The method of Wang *et al.*[10] involved the use a Si wafer to screen the actual substrate from the plasma during CNT growth from a thin Fe film at high temperature (~850 °C).

In this work, we demonstrate shielded growth of CNTs and CNFs from nearly monodispersed Fe_2O_3 nanoparticles at low substrate temperatures using plasma powers in the range of 200–500 W. For the first time, we demonstrate the use of microwave shielding to control the selectivity of carbon nanostructures at low temperatures. Fig. 1 illustrates the experimental setup used for the growth of CNTs/CNFs at low temperatures from exposed and shielded Fe_2O_3 nanoparticles. The minimum substrate temperatures for the growth of CNTs and CNFs were 400 and 200 °C, respectively. At 400 °C, both CNTs and CNFs were simultaneously grown from shielded and exposed catalysts, respectively. The Fe_2O_3 nanoparticles were obtained by interdendritic stabilization of Fe^{3+} ions and subsequent calcination of the resulting nanocomposite.

An amine-terminated fourth-generation poly(amidoamine) (PAMAM) dendrimer having an ethylenediamine core (G4-NH_2) was purchased as a 10% methanol solution from Aldrich. Prior studies[11,12] have shown that dendrimers can serve as good 'nanotemplates' for the controlled and reproducible synthesis of transition metal nanoparticles. In particular, an amine-terminated dendrimer can be easily immobilized on solid surfaces because of the presence of a reactive handle, which serves as a link.[12] The Fe^{3+}/G4-NH_2 composite was synthesized according to a recipe described by Fahlman and coworkers.[13] The G4-NH_2 dendrimer (0.4156 g, 0.12 mmol) and $FeCl_3{\cdot}6H_2O$ (0.5123 g, 1.89 mmol) were separately dissolved in 20 mL of deionized water and stirred for 10 min. Both solutions were combined and stirred vigorously for 4 h resulting in the formation of dendrimer-stabilized Fe^{3+} nanocomposite. Before dip coating, the SiO_2 (1 μm)-coated Si substrate substrates were washed several times with distilled water,

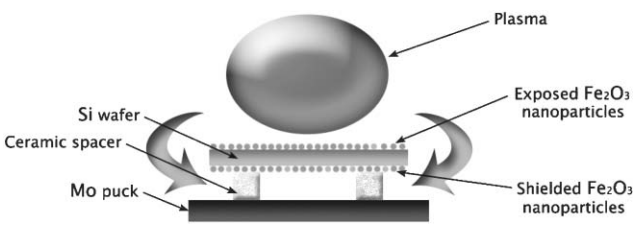

Fig. 1 Schematic of experimental setup for low-temperature growth of CNTs from shielded and exposed SiO_2/Si-supported Fe_2O_3 nanoparticles in the PECVD reactor (not to scale). Plasma powers were in the range of 200–500 W.

[a]*Birck Nanotechnology Center, Discovery Park, Purdue University, West Lafayette, IN, 47907, USA. E-mail: pamama@purdue.edu; Fax: 765-494-1204; Tel: 765-494-0145*
[b]*Department of Chemistry, Alabama A&M University, Normal, AL, 35762, USA*
[c]*School of Mechanical Engineering, Purdue University, West Lafayette, IN, 47907, U.S.A*
[d]*School of Materials Engineering, School of Electrical & Computer Engineering, Purdue University, West Lafayette, IN, 47907, U.S.A*
† Electronic supplementary information (ESI) available: AFM image of mica-supported Fe_2O_3 nanoparticles and topographic height profile for the nanoparticles. See DOI: 10.1039/b602623k

ethanol, and then dried under a stream of N_2 gas. The composite was immobilized on the substrates by dip coating for 10 s, and drying in N_2. The immobilized Fe^{3+}/G4-NH_2 was calcined at 250 °C for 20 min to remove the organic dendrimer, leaving behind nearly monodispersed Fe_2O_3 nanoparticles.

Reaction conditions employed were determined from a previous optimization study for SWNT growth over Mo/Co catalyst supported on nanoporous MgO.[14] A detailed description of the PECVD system and growth procedure is also reported therein. The catalyst was annealed in an N_2 atmosphere to the reaction temperature to enhance the stabilization of the Fe_2O_3 nanoparticles. At reaction temperature, a H_2 plasma was initiated using 200–500 W, and a hydrogen (50 sccm)/methane (10 sccm) mixture was maintained for 20 min. The as-synthesized carbon products were characterized using an Hitachi S4800 field emission gun scanning electron microscope (FESEM) and a JEOL JEM-2000FX transmission electron microscope (TEM). Raman spectroscopic measurements of the products were also performed using a Renishaw Raman imaging microscope with a 785 nm (1.58 eV) laser as the excitation source. Each spectrum obtained was an average of four spectra acquired from multiple spots on the sample.

Characterization of the catalytic template by atomic force microscopy (AFM) and FESEM revealed that the Fe_2O_3 nanoparticles were nearly monodispersed on the substrate and predominantly less than 10 nm in size,[15,16] which suggest that a large percentage of nanoparticles were within the size range selective for CNT growth. An AFM image of mica-supported Fe_2O_3 nanoparticles and a corresponding topographic height profile for nanoparticles along the reference line are presented in the ESI.† The AFM image reveals well dispersed Fe_2O_3 nanoparticles (mean size = 3.7 $\pm$ 0.95 nm) after 10 s of dip coating in the Fe^{3+}/G4-NH_2 solution and calcination at 250 °C. Detailed characterization of the dendrimer-stabilized Fe nanoparticles is reported elsewhere.[16]

The Fe_2O_3 nanoparticles were highly susceptible to coarsening in the PECVD growth environment, resulting in either CNT non-selectivity or decreased catalytic activity. For successful low-temperature growth of CNTs by PECVD using Fe_2O_3 nanoparticles, in addition to shielding the catalyst, catalysts were annealed in N_2 and pretreated in H_2 for <5 min to promote the stabilization and generate a high density of active catalytic sites. A study involving the effect of annealing ambient on the catalytic activity of Fe nanoparticles in the PECVD revealed that the stabilization of the catalyst is enhanced in an N_2 environment.[16] Prolonged H_2-prereduction (>5 min) also increased coarsening of catalytic particles.

Growth at low-temperatures using Fe_2O_3 nanoparticles immobilized on both sides of SiO_2-coated Si substrates (Fig. 1) revealed a dramatic difference in CNT selectivity for the catalyst exposed to the plasma (top side of the substrate) and the catalyst shielded from the plasma (back side of the substrate). As presented in the FESEM and TEM images in Fig. 2, reactions conducted at a substrate temperature of 400 °C and plasma power of 500 W (Fig. 2(a) and (c)) yielded CNFs and CNTs for the exposed and shielded catalysts, respectively. TEM characterization was performed on the CNTs/CNFs obtained from the shielded catalysts to confirm the structures. Following ultrasonic treatment in ethanol, the nanostructures were transferred to a TEM carbon grid. Fig. 2(c) shows an image of a MWNT grown at 400 °C with many catalytic particles around it.

The diameters of most CNTs ranged from 10 to 30 nm, with few CNTs in the 100 nm range, and typical lengths ranged from 500 nm to several microns. The minimum growth temperature achieved for CNFs was 200 °C (Fig. 2(b) and (d)) using the shielded growth approach. Fig. 2(d) shows a TEM image of a CNF with encapsulated catalytic particles grown from the shielded catalyst at 200 °C and plasma power of 500 W. The low density of CNTs/CNFs observed in the TEM images is due to the strong adhesion of CNTs/CNFs to the substrate and the difficulty in removing them during sonication.

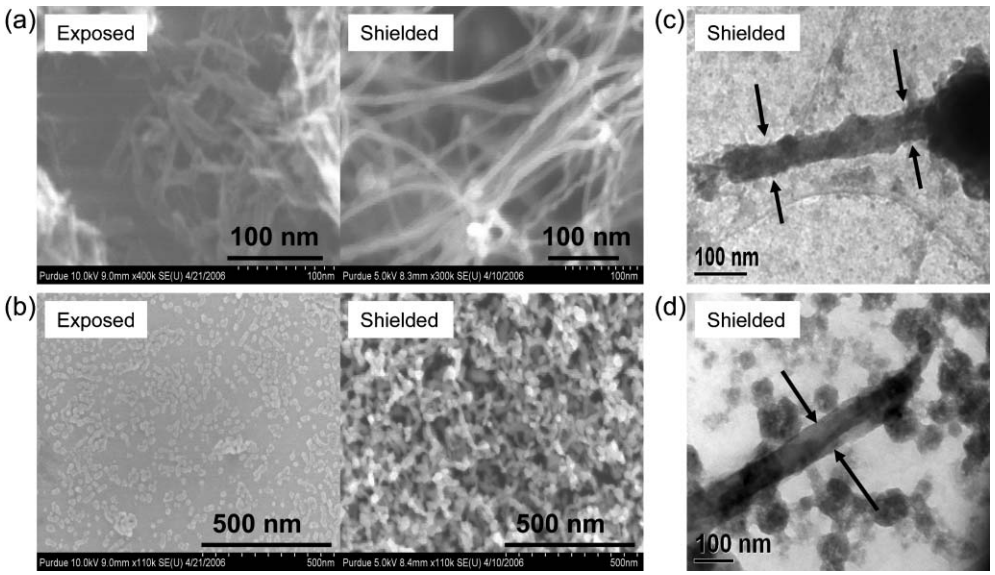

Fig. 2 FESEM and TEM characterization of carbon nanostructures produced at 400 and 200 °C using microwave PECVD at 500 W power, 10 sccm CH_4/50 sccm H_2 flow rate and reaction time of 20 min. (a) FESEM images of CNFs and CNTs grown from exposed and shielded Fe_2O_3 nanoparticles at 400 °C, respectively. (b) FESEM images of CNFs/CNTs grown from exposed and shielded Fe_2O_3 nanopartilces at 200 °C. TEM images of CNTs grown from shielded Fe_2O_3 nanoparticles at (c) 400 °C and (d) 200 °C.

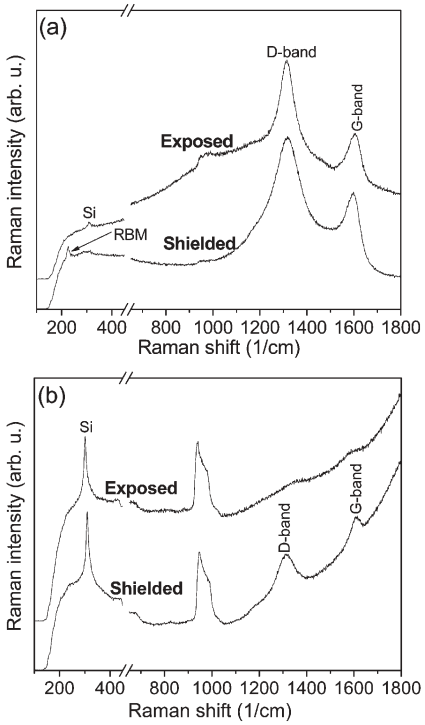

Fig. 3 Raman spectra of carbon nanostructures grown from exposed and shielded Fe_2O_3 nanoparticles at (a) 400 °C and (b) 200 °C.

Raman spectroscopy is a powerful tool for the characterization of SWNTs because of the strong coupling that exists between phonons and electrons in CNTs.[17] The G-band occurring near 1590 cm^{-1} originates from the in-plane stretching mode of the graphene sheets. The D-band, which occurs near 1310 cm^{-1} is associated with the presence of amorphous carbon and defects in graphene sheets. The presence of the radial breathing mode (RBM) in the lower frequency region is strong evidence that the carbon material contains SWNTs. From the RBM frequency (ω_{RBM}), the diameter of the SWNT can be determined using the relation ω_{RBM} (cm^{-1}) = 12.5 + 223.5/d (nm).[18]

Fig. 3(a) and (b) show the Raman spectra of the as-synthesized carbon nanostructures grown from the shielded and exposed catalyst nanoparticles at 400 and 200 °C, respectively. All spectra except for products obtained from the exposed catalyst at 200 °C exhibit distinct D and G bands, indicating the presence of amorphous carbon and CNTs/CNFs. The FESEM images shown in Fig. 2(a) and (b) are consistent with this observation. The appearance of an RBM peak at 224 cm^{-1} provides strong evidence that SWNTs were grown from the shielded catalyst at 400 °C. The absence of low-frequency RBM peaks for carbon products obtained from the exposed catalyst indicates that SWNTs were not grown. On the basis of the equation given above, the diameter of SWNTs grown from the shielded catalyst is estimated to be ~1.1 nm. However, this estimate does not preclude the existence of other SWNT diameters because of the strong resonant enhancement effect, whereby the RBM peaks vary with the laser excitation energy.[10]

The exposed catalyst nanoparticles showed low selectivity to CNT/CNF formation at 200 °C, evidenced by the absence of well defined D and G bands in the Raman spectrum presented in Fig. 3 and the FESEM image in Fig. 2(b). Conversely, the Raman spectrum of the products from the shielded catalyst exhibits distinct D and G bands, indicating the formation of carbon products, mainly CNFs as suggested by FESEM and TEM studies. Low-frequency RBM peaks are not observed in Fig. 3(b), which suggests the absence of SWNTs in this sample. The broadened G-band peak and the low ratio of the intensity of the G-band with respect to the D-band observed in all the Raman spectra suggests the presence of defects, amorphous carbon and poor crystallinity of the CNTs/CNFs.

In summary, low-temperature growth of CNTs by PECVD has been demonstrated using a shielded synthesis approach involving exposed, nearly monodispersed Fe_2O_3 nanoparticles annealed in an N_2 atmosphere. We have shown for the first time that microwave shielding can be used to control the selectivity of carbon nanostructures during PECVD growth. To increase selectivity to SWNTs at 400 °C, we are currently studying the shielded growth mechanism and determining an appropriate method of removing the dendrimer without significantly increasing the particle size distribution.

This research is supported by the NASA-Purdue Institute for Nanoelectronics and Computing and the Birck Nanotechnology Center. We thank Vijay Rawat for assistance with TEM imaging.

Notes and references

1 S. Iijima, *Nature*, 1991, **354**, 56.
2 A. V. Melechko, V. I. Merkulov, T. E. McKnight, M. A. Guillorn, K. L. Klein, D. H. Lowndes and M. L. Simpson, *J. Appl. Phys.*, 2005, **97**, 041301.
3 M. S. Dresselhaus, G. Dresselhaus and P. C. Eklund, *Science of Fullerenes and Carbon Nanotubes*, Academic Press, New York, 1996.
4 S. Hofmann, C. Ducati, J. Robertson and B. Kleinsorge, *Appl. Phys. Lett.*, 2003, **83**, 135.
5 (*a*) E. J. Bae, Y.-S. Min, D. Kang, J.-H. Ko and W. Park, *Chem. Mater.*, 2005, **17**, 5141; (*b*) B. Kleinsorge, V. B. Golovko, S. Hofmann, J. Geng, D. Jefferson, J. Robertson and B. F. G. Johnson, *Chem. Commun.*, 2004, 1416; (*c*) H. S. Uh and S. S. Park, *J. Electrochem. Soc.*, 2004, **151**, H164; (*d*) B. O. Boskovic, V. Stolojan, R. U. A. Khan, S. Haq and S. R. P. Silva, *Nat. Mater.*, 2002, **1**, 165; (*e*) B. D. Yao and N. Wang, *J. Phys. Chem. B*, 2001, **105**, 11395.
6 W. L. Wang, X. D. Bai, Z. Xu, S. Liu and E. G. Wang, *Chem. Phys. Lett.*, 2006, **419**, 81.
7 B. B. Wang, S. Lee, X. Z. Xu, S. Choi, H. Yan, B. Zhang and W. Hao, *Appl. Surf. Sci.*, 2004, **236**, 6.
8 Y. Shiratori, H. Hiraoka and M. Yamamoto, *Mater. Chem. Phys.*, 2004, **87**, 31.
9 Y. Min, E. J. Bae, B. S. Oh, D. Kang and W. Park, *J. Am. Chem. Soc.*, 2005, **127**, 12498.
10 Y. Y. Wang, S. Gupta and R. J. Nemanich, *Appl. Phys. Lett.*, 2004, **85**, 2601.
11 H. C. Choi, W. Kim, D. Wang and H. Dai, *J. Phys. Chem. B*, 2002, **106**, 12361.
12 R. W. J. Scott, O. M. Wilson and R. M. Crooks, *J. Phys. Chem. B*, 2005, **109**, 692.
13 J. K. Vohs, J. J. Brege, J. E. Raymond, A. E. Brown, G. L. William and B. D. Fahlman, *J. Am. Chem. Soc.*, 2004, **126**, 9936.
14 M. R. Maschmann, P. B. Amama, A. Goyal, Z. Iqbal, R. Gat and T. S. Fisher, *Carbon*, 2006, **44**, 10.
15 P. B. Amama, M. R. Maschmann, T. S. Fisher and T. D. Sands, *Abstract of Papers, 230th ACS National Meeting*, Washington, DC, 2005. INOR-065. CODEN: 69HFCL AN 2005:739017.
16 P. B. Amama, M. R. Maschmann, T. S. Fisher and T. D. Sands, *J. Phys. Chem. B*, 2006, DOI: 10.1021/jp057302d.
17 M. S. Dresselhaus and P. C. Eklund, *Adv. Phys.*, 2000, **49**, 705.
18 S. M. Bachilo, M. S. Strano, C. Kittrell, R. H. Hauge, R. E. Smalley and R. B. Weisman, *Science*, 2002, **298**, 2361.